Mesoanalysis of the Big Thompson Storm

FERNANDO CARACENA, ROBERT A. MADDOX, L. RAY HOXIT AND CHARLES F. CHAPPELL

Atmospheric Physics and Chemistry Laboratory, NOAA, Boulder, CO 80302

(Manuscript received 3 April 1978, in final form 8 September 1978)

ABSTRACT

Mesoscale analyses and descriptions of meteorological conditions that produced the devastating flash flood in the Big Thompson Canyon on 31 July 1976 are presented. The storm developed when strong low-level easterly winds to the rear of a polar front pushed a moist, conditionally unstable air mass upslope into the Front Range of the Rocky Mountains. The main thrust of the moisture flux focused initially into the Big Thompson area. Orographic uplift released the convective instability, and light south-southeasterly winds at steering levels allowed the storm complex to remain nearly stationary over the foothills. Heavy rains fell within the storm along a narrow corridor only 5 km wide oriented north-northeast by south-southwest. Minimal entrainment of relatively moist air at middle and upper levels, very low cloud bases and a slightly tilted updraft structure contributed to a high precipitation efficiency. A deep warm layer of convective cloud fostered precipitation growth through warm cloud processes. The greatest concentrations of precipitation size particles remained at low elevations and as a result of poor vertical beam resolution returned anomalously weak radar echoes to a WSR-57 located 110 n mi away.

1. Introduction

A large quasi-stationary thunderstorm complex formed over the Big Thompson river drainage west of Loveland, Colorado, on the evening of 31 July 1976. Intense rainfall produced devastating flash floods leaving at least 139 dead and $35.5 million in property damage. The thunderstorm complex that caused the flash flood is hereafter referred to as the Big Thompson storm.

Several scales of atmospheric motion interacted to focus the intense convection in the foothills from west of Boulder to northwest of Fort Collins. Maddox *et al.* (1977, 1978) presented a detailed analysis of the meteorological conditions which culminated in the Big Thompson floods. Briefly they are as follows:

1) At upper levels (500–300 mb) the flow around a negatively tilted ridge was light southeasterly over the Front Range area of Colorado.

2) A short-wave trough on the meso-α scale (at 500 mb) was approaching the region from the south along the west side of the ridge.

3) A polar airmass lay to the northeast of the Front Range, with the polar front stretching across southeastern Colorado.

4) During the day, increasing surface pressure over Nebraska and northeastern Colorado, and falling pressure over northwestern Colorado, accelerated a secondary cold frontal surge that reached the foothills of the Front Range about 0000 GMT 1 August 1976.[1]

5) Behind the secondary cold front, a deep moist flow in the boundary layer carried potentially very unstable air upslope. The strong moisture intrusion focused on the Big Thompson area.

This study concerns the following mesoscale meteorological features and cloud microphysical aspects of the storm: 1) local-scale surface conditions preceding and during the formation of the Big Thompson storm, 2) history of the storm portrayed by its radar echoes 3) radar-inferred temporal and spatial distributions of rainfall, 4) moisture budget and precipitation efficiency of the storm and 5) physical structure of the storm complex.

2. Local analysis

Surface data were available from the following sites along the Front Range: Ft. Collins (Colorado State University, Atmospheric Science Building), Greeley (University of Northern Colorado, Ross Hall), Table Mountain (NOAA-ERL[2]), Boulder (NOAA-ERL), Golden (Colorado School of Mines), Jefferson County Airport (FAA[3]), Rocky Flats

[1] All times in this paper are Greenwich Mean Time (GMT) on 31 July and 1 August 1976, unless specified otherwise.

[2] National Oceanic and Atmospheric Administration (NOAA), Environmental Research Laboratory (ERL).

[3] Federal Aviation Administration (FAA).

(ERDA[4]), Denver (Stapleton International Airport, NOAA-NWS[5]) and Arapahoe County Airport (FAA).

At three sites (Stapleton International Airport, Table Mountain and Rocky Flats) surface data were recorded on an almost continuous basis. At Table Mountain (~6 mi north of Boulder) the east–west component of the wind was measured, from the surface to 600 m, with a Doppler acoustic echosounder operated by the Wave Propagation Laboratory of NOAA-ERL.

Data from the above sources, together with NWS radar data from Limon, Colorado, were used in constructing the local-scale surface analyses shown in Fig. 1. The progress of the second cold front into the Front Range area and its interaction with existing thunderstorms is shown. In the Ft. Collins, Loveland, and Greeley areas an increase in wind speeds and gustiness were the only indications of the passage of the trailing cold front. These areas had remained partly cloudy with upslope southeasterly flow during the afternoon, resulting in little surface temperature change across the front. In the Denver-Boulder area, however, afternoon cloudiness was minimal. The resulting heating and mixing had elevated surface temperatures and lowered surface dewpoints. Winds were also more southerly. The cold front passed Stapleton and Table Mountain (see Figs. 2 and 3) at about 2330. At both of these sites, the passage was accompanied by a significant increase in easterly or southeasterly winds. Dewpoint temperatures increased 5.5–7°C (10–13°F) and temperatures dropped 5.5–6.5°C (10–12°F) in a 30 min period.

Prior to 2330 a large thunderstorm had developed along the higher terrain southeast of Stapleton International Airport near Denver as the trailing front moved into this region. This storm moved northwestward and merged with cells that formed between 2330–0000 ahead of the front in the region west of Denver. The resulting arc of echoes (see Fig. 1) moved into the Boulder area around 0030.

A gust front and clouds of blowing dust were associated with this line of thundershowers. A strong cell moved across Rocky Flats where a time series (Fig. 4) shows that wind gusts to 21 m s^{-1} (41 kt) occurred about 0015 just ahead of a brief but heavy rainshower. Temperature and dewpoint temperature changes here were comparable to those at Stapleton and Table Mountain.

Eyewitness accounts and the 0000 rawinsonde data (see Figs. 5a and 5b) indicate that the clouds in the prefrontal air mass had higher bases than those in the postfrontal air mass. Between 0030 and 0100 pressure rises of about 1 mb were observed at Rocky Flats, Boulder and Golden. These pressure changes were accompanied by a wind shift to the southwest. Evidently, rain showers and evaporative cooling in drier air along the foothills between Boulder and Golden had produced a small meso-high pressure area. The winds at both Boulder and Rocky Flats remained light southerly to westerly until about 0400.

That portion of the arc of echoes east of Boulder dissipated rapidly after 0030 GMT, while the western portion moved over the foothills southwest of Boulder. Here rainfall amounts were much less than those observed 30–130 km (20–80 mi) to the north. Moreover, the echoes west and south of Boulder moved westward almost to the Continental Divide, indicating that they were not strongly affected by the terrain. It seems likely that the trailing front became quasi-stationary between Denver and the foothills south of Boulder. Therefore, the very moist, unstable air behind the front probably did not reach the elevated terrain southwest of Boulder.

From Boulder northward, meteorological conditions were very different. The trailing front moved into the foothills shortly after 2330, and convective clouds developed very rapidly. By 0000 a few echoes were detected by radar, and by 0030 several strong thunderstorms were oriented in a north–south line along the foothills. Many residents of the Ft. Collins, Loveland and Longmont areas reported strong east-southeasterly winds and low clouds moving rapidly into the foothills. Cloud bases were estimated to be at 2.2–2.7 km (7000–9000 ft) MSL.

The second front developed a westward bulge from Boulder to Fort Collins (see Fig. 1) as it approached the Front Range. Radar echo motions indicate that the area of this bulge was also an area of most rapid cell propagation toward the west. The echo motions were determined by using National Hail Research Experiment (NHRE) radar data from Grover, Colorado. The average velocity vectors of echo centroids (>45 dBZ) for the period from 0030 to 0100 are shown in Fig. 6. Superimposed on this figure is the 0000 local surface analysis from Fig. 1. North of Storm Mountain echo motion was northward at 8–10 m s^{-1}. In the Big Thompson area, however, echo motion was from the southeast (120–150° azimuth) at 8–12 m s^{-1}. Although portions of the storm south of Lyons were beyond Grover radar range, one large distinct cell could be followed on Limon radar. This cell, near Table Mountain, propagated westward at 5 m s^{-1}. The pattern of cell motions and the orientation of the cold front suggest an enhanced easterly flow in the boundary layer with a strong moisture flux into the Big Thompson area.

Data taken at Table Mountain sampled this region of strong easterly inflow. After the passage of the cold front the easterly component of the wind

[4] Energy Research and Development Administration (ERDA).
[5] National Weather Service (NWS).

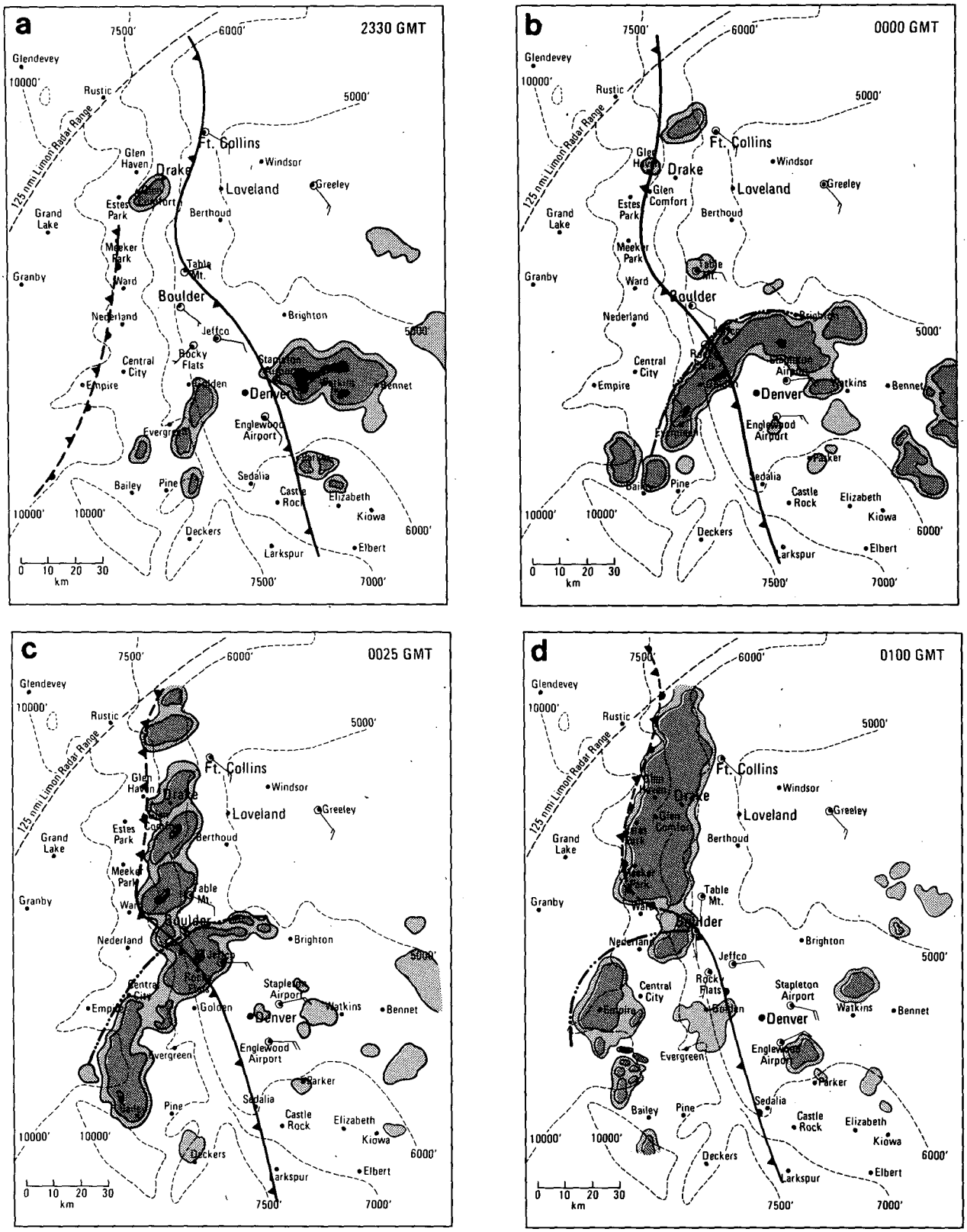

FIG. 1. Local-scale surface analyses. Frontal positions and reported winds are in black; Limon radar echoes are shown with VIP level 1 return shaded light gray, level 2 shaded medium gray and level 3 shaded dark gray. (a) 2330 GMT 31 July 1976, (b) 0000 GMT 1 August 1976, (c) 0025 GMT 1 August 1976, (d) 0100 GMT 1 August 1976.

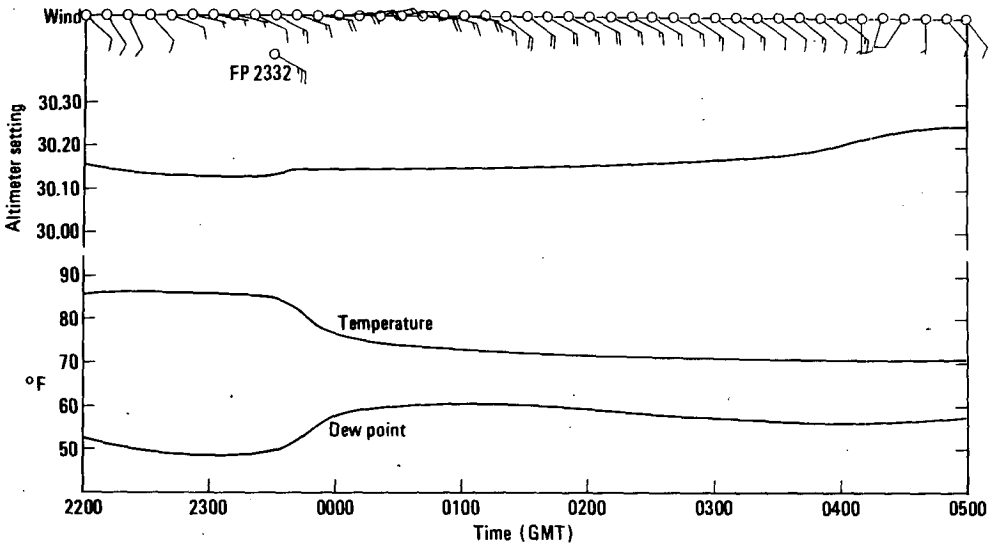

FIG. 2. Time series plots of surface wind (kt), altimeter setting (inches of mercury), and temperature and dewpoint temperature (°F) as recorded at Stapleton International Airport, Denver. Time covered is from 2200 GMT 31 July 1976 to 0500 GMT 1 August 1976.

exceeded 20 m s^{-1} at 400–600 m above the surface. As the weakening gust front (shown in Fig. 1) moved northward over Table Mountain around 0100, the easterly flow in the lower 200 m was temporarily interrupted. Over the next 20 min the intensity of echoes over the Big Thompson decreased dramatically apparently due to the modification of the storms' inflow by the gust front.

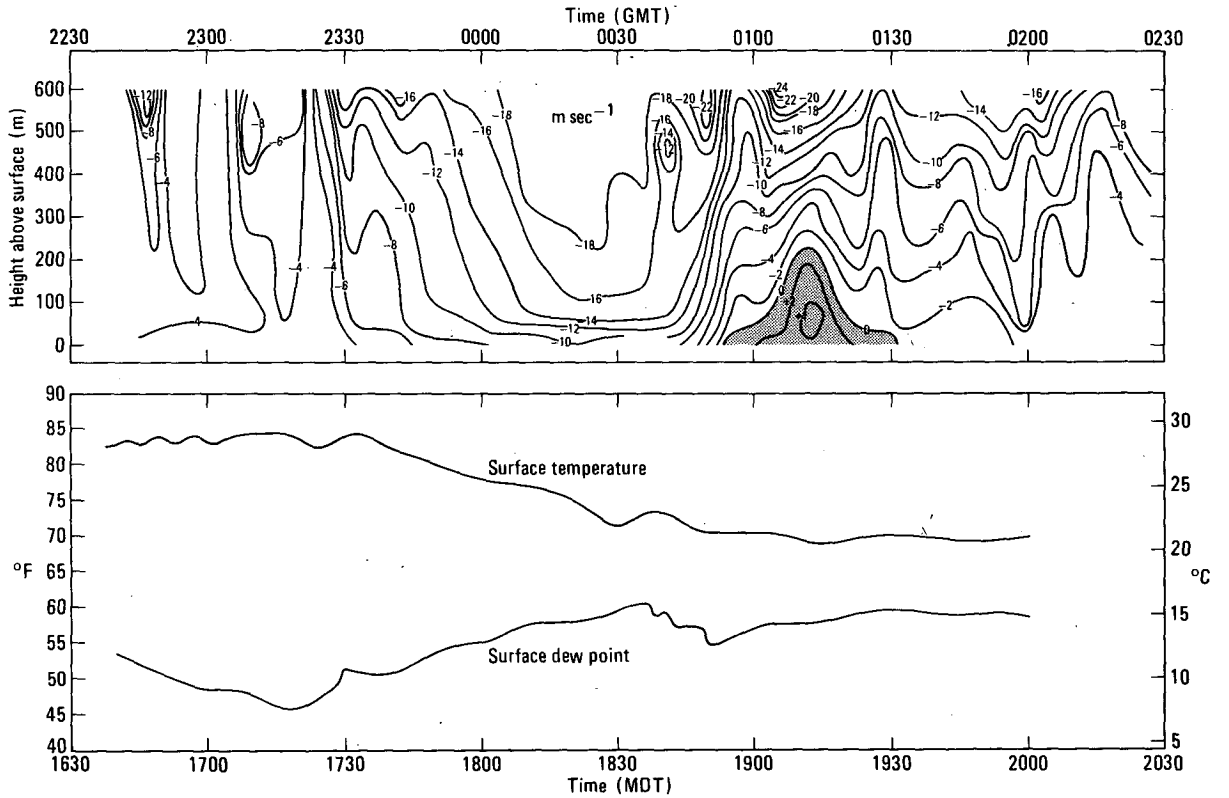

FIG. 3. Time series of east-west component of wind (m s^{-1}), temperature and dewpoint temperature (°F) from the Wave Propagation Laboratory site on Table Mountain modified from an original analysis by Pratt (1977, private communication). Negative values indicate easterly winds. Occurrence of light westerly winds near the surface is denoted by gray shading. Time covered extends from 2230 GMT 31 July 1976 to 0230 GMT 1 August 1976.

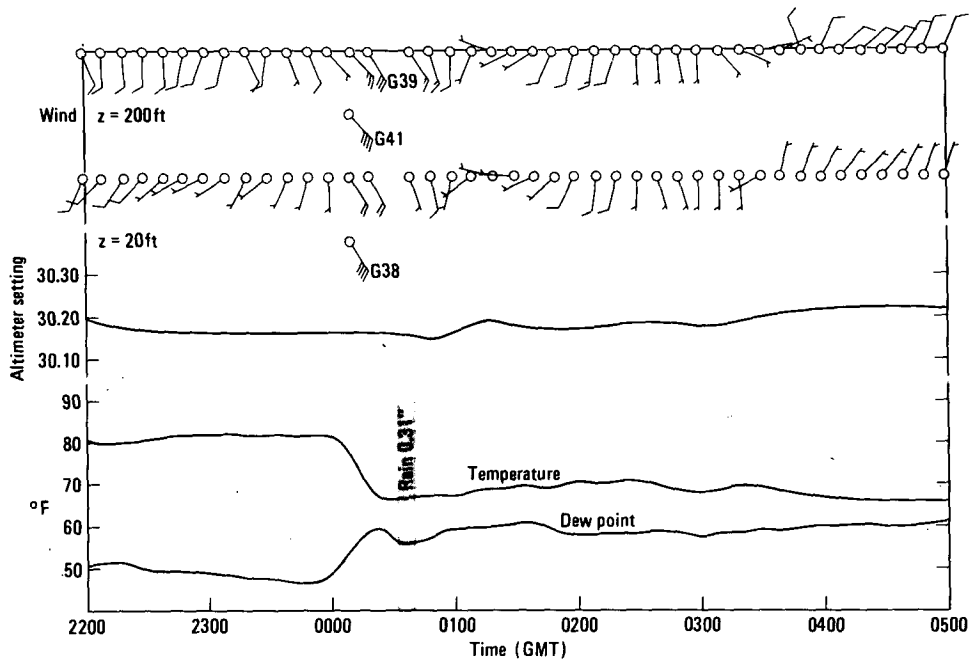

FIG. 4. Time series plots (similar to Fig. 2) for Rocky Flats, Colorado. Winds were measured at 20 and 200 ft AGL on an instrumented tower.

The Denver 0000 sounding (Fig. 5a), released at 2315 in the prefrontal air mass, and a postfrontal sounding interpolated for Loveland, (Fig. 5b) show that both air masses were potentially unstable. The lifted index (LI) computed from the Denver sounding was −2. The corresponding value for the Loveland sounding was −6, reflecting the very moist conditions between the surface and 730 mb (mean mixing ratio 14.8 g kg^{-1}).

The prefrontal air mass contained a dry adiabatic lapse rate from the surface to 590 mb, and with a level of free convection (LFC) at 620 mb, thunderstorms could readily form in this airmass during the afternoon. The postfrontal air mass, however, was strongly capped by a frontal inversion at 730 mb, which was also the height of the lifted condensation level (LCL). An additional 80 mb of lift was necessary to bring this air mass to its LFC and release its strong potential instability. This additional lifting was realized as the airmass moved up into the foothills. Meanwhile, nocturnal cooling over the plains extinguished any remaining convection east of the Front Range. A steady inflow into the storm was established and continued to feed the quasi-stationary Big Thompson Storm.

3. Radar coverage of the storm

Two 10 cm meteorological radars scanned the storm for portions of its lifetime. The combined data from these two radars yields a complete history of the storm's evolution.

A WSR-57 operated by the National Weather Service (NWS) at Limon, Colorado, was situated approximately 205 km southeast of the storm area. Because of its 2° conical beam width, a 1 km pulse length and large distance from the storm area, it was not able to resolve individual cells unless they were isolated, intense and very large. The pulse volume of Limon radar in the storm area was about 40 km^3. Temporal resolution was excellent since PPI scope photographs (at 0° elevation) were made about every 2 min.

A research radar at Grover, Colorado, about 115 km east-northeast of the storm area, was operated by the National Center for Atmospheric Research. It provided excellent spatial and temporal coverage of the first hour of the storm's lifetime. Its shorter distance from the storm area combined with its narrower beam (1° conical beamwidth) and smaller pulse length (300 m) allowed a much better resolution of storm structures than Limon radar (down to ~1 km^3). Grover radar also made three-dimensional scans of the storm with a cycle time of about 2 min. Unfortunately, interrogation of the storm complex was terminated at about 0100, prior to the period of major flooding.

Limon and Grover radar reflectivities, through approximately the same horizontal section of the storm (4.5–6.1 km MSL at 0045), are shown superimposed in Fig. 7. This figure shows that Limon radar provided rather poor resolution of the storm's reflectivities in two ways: 1) in the intensity of the radar cores and 2) in the size of the weaker portions

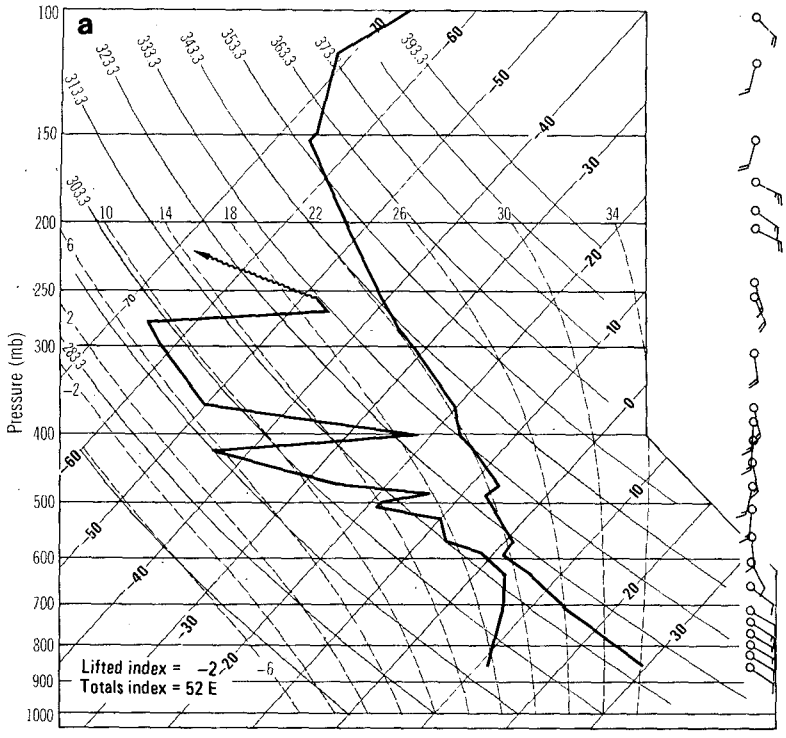

FIG. 5a. Skew T/log P plot of 0000 GMT 1 August 1976, Denver upper air sounding.

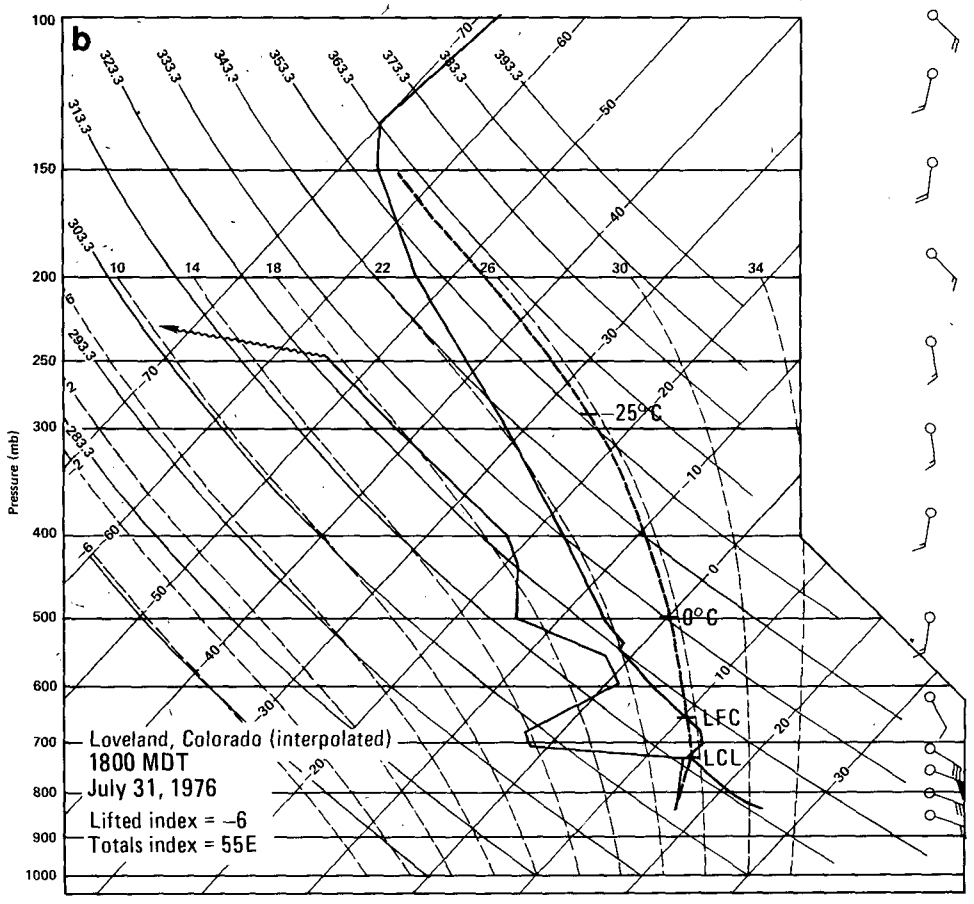

FIG. 5b. Skew T/log P plot of upper air sounding constructed for Loveland, Colorado, 0000 GMT 1 August 1976. LCL and LFC levels and moist adiabat are shown for a lifted parcel with mean thermodynamic characteristics of lowest 100 mb layer.

of the echo. Limon radar indicated a maximum possible reflectivity of about 46 dBZ in the high reflectivity cores, whereas Grover radar contoured these areas as exceeding 55 dBZ with measured maxima of about 65 dBZ. Fig. 7 also shows that the indicated Limon VIP level 2 threshold extended a few kilometers beyond the 15 dBZ contour indicated by Grover radar.

Both Limon and Grover radar data contain gaps in temporal coverage of the Big Thompson storm; Grover radar, because its coverage of the storm was terminated too soon, and Limon radar, because early coverage of the storm was interrupted to make extensive cloud-top measurements in south-

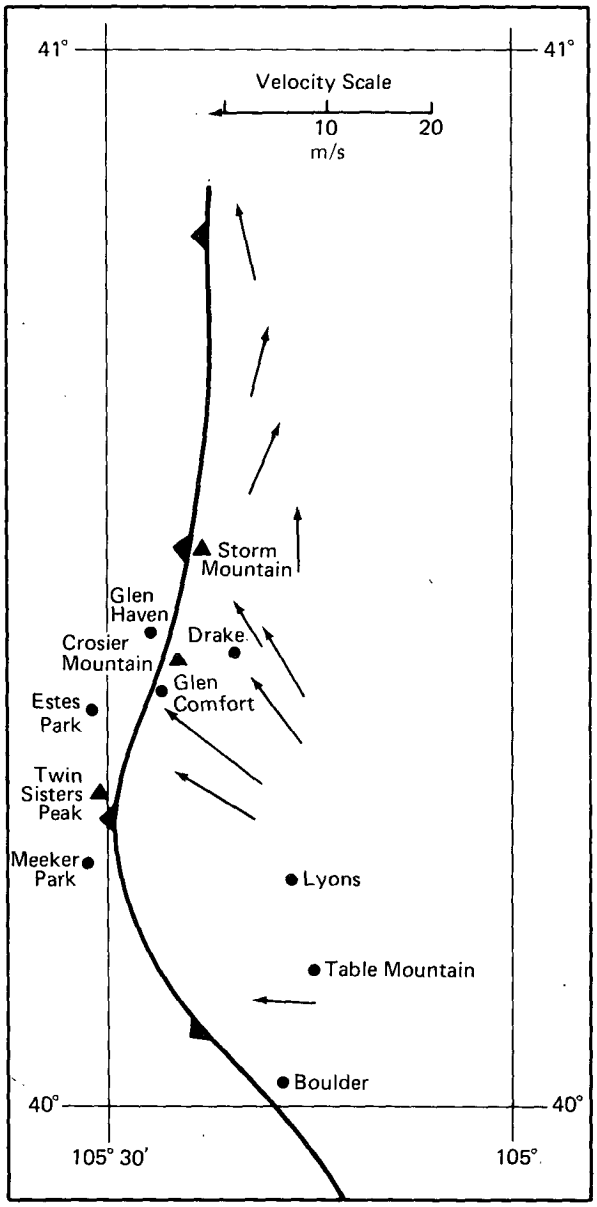

FIG. 6. Velocities of identifiable radar echo cores in 3.3° PPI elevation scans made by Grover radar along the Front Range during the period 0030–0100 GMT.

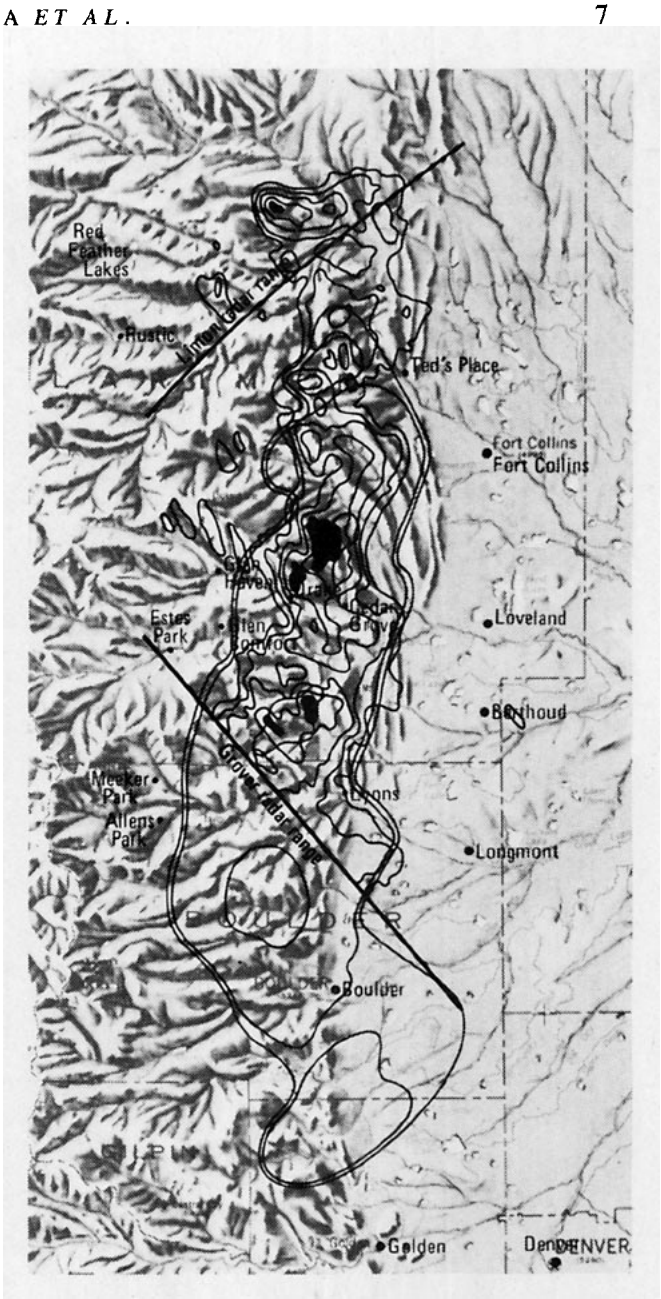

FIG. 7. Relief map showing 0045 GMT radar echoes from NWS radar at Limon, Colorado (Gray), and from NHRE radar at Grover, Colorado (black). Limon contours are for VIP levels 1, 2 and 3 thresholds, which correspond to the minimum detectable signal, 30 dBZ and 41 dBZ, respectively. VIP level 4 which has a threshold of 46 dBZ did not contour at this time. Grover contours are at 10 dBZ intervals beginning at 15 dBZ with regions of reflectivity ≥55 dBZ shaded black.

eastern Colorado. However, the combined radar time series yields an unbroken history of the storm's evolution. A composite-echo time series based on the two radars is presented in Fig. 8. In order to maintain continuity, Limon radar's indicated VIP level 2 contour was used as the outline of the storm where it was available. To resolve individual cells, Limon radar echo cores (VIP level 3 and higher) were replaced by Grover radar echo cores (>35 dBZ) where available.

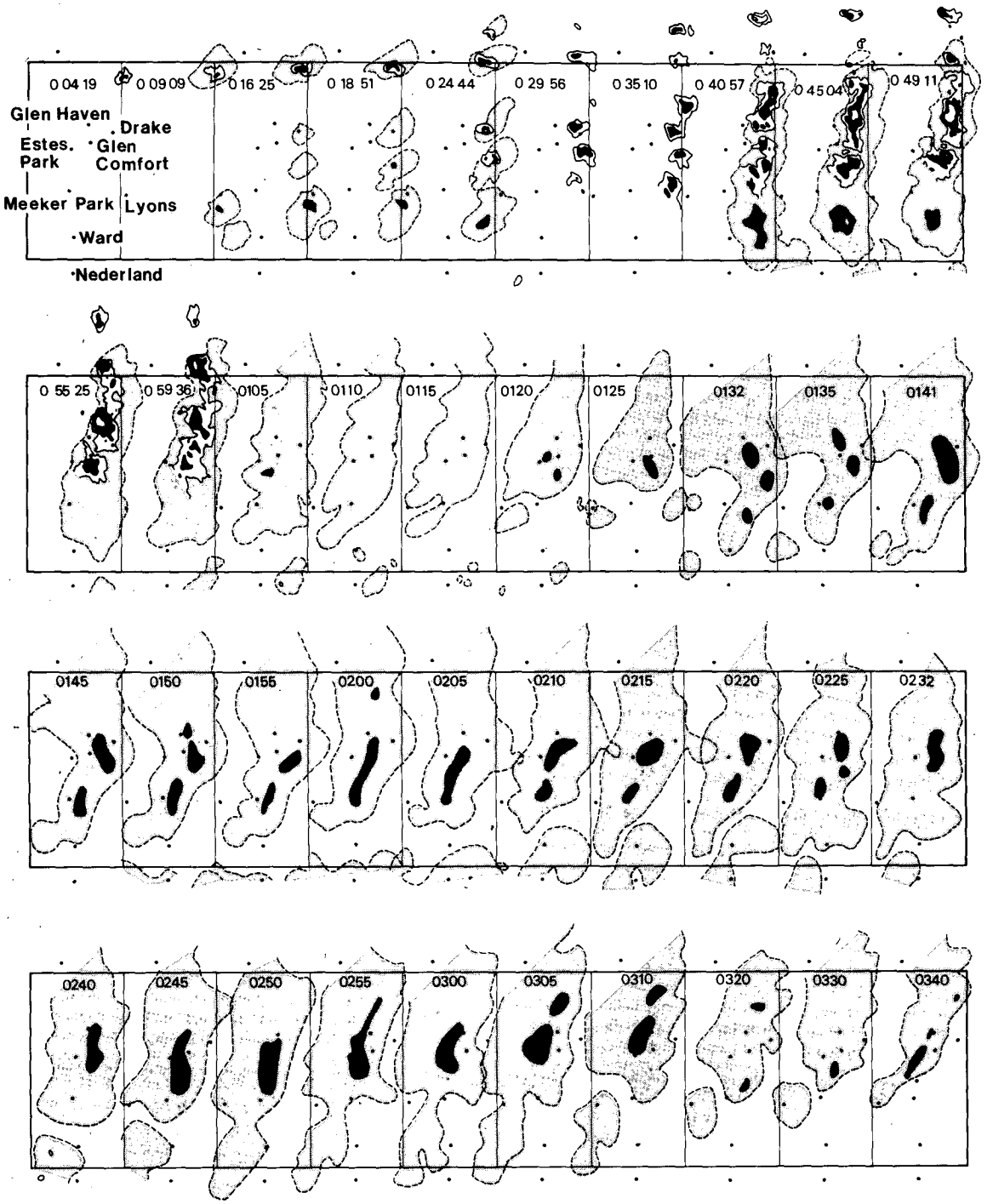

FIG. 8. Composite-echo time series formed from both Limon and Grover radar echoes showing the evolution of the storm from 0004 to 0340 GMT 1 August 1976. Light gray shading corresponds to Limon VIP level 2 (where available). 35 dBZ contours and higher (alternating white and black at 10 dBZ increments) from Grover radar over the period 0004–0059 replace Limon VIP levels 3 and higher. Where Grover data are available time is presented in the format hours (0), minutes and seconds.

Fig. 8 shows that the storm complex was generated by the merger of a number of westward moving cells which formed over the foothills along a north-south axis running between Lyons and Drake. The greater easterly component of cell motion south of Drake is evidenced by the progressive change in orientation of the echo complex between 0000 and 0100. Cells just east of Meeker

Park advanced more rapidly westward than those to the north and south producing a bowed structure in the echo complex.

During the period of cell merger storm reflectivities increased rapidly, reaching a peak at about 0045. Echo intensities then subsided until 0120 when the storm complex began to reintensify. During the period from 0130 to 0310 the storm complex remained nearly stationary along a narrow corridor extending from just east of Meeker Park to a point just northeast of Glen Haven.

Although not resolved by Limon radar, the data suggests that new convective cells repeatedly formed over the mountains south-southeast of Glen Comfort and tracked north-northwestward toward Glen Haven. Around 0230 the heavy rain shifted slightly westward into the area between Estes Park and Glen Haven producing flash flooding in the creeks that drain this area.

4. Storm scale analysis

The composite-echo time series presented in Fig. 8 was used as a basis for estimating rainfall distributions in space and time, computing mass rainout rates and estimating the storm precipitation efficiency.

a. Rainfall rates

Fig. 7 clearly shows that areas of VIP level 3, indicated by Limon radar, corresponded fairly well with reflectivity core areas with a range 55–65 dBZ as indicated by Grover radar. Although Limon radar data can be used to identify the areas of the storm which produced heavy rain, its indicated reflectivities were too low in these areas. The discrepancy between a maximum possible reflectivity of 46 dBZ indicated by Limon radar and 55–65 dBZ contoured within these same areas by Grover radar translates into about an order of magnitude error in computed rainfall rates. In order to correct for this error, use was made of a time series of storm reflectivities (from Fig. 8) over a site which was affected by some of the heaviest rain, Glen Comfort. Indicated reflectivities were converted into rainfall rates (R) by means of a Z–R relationship. A multiplicative factor was found that normalized the radar-computed rainfall to the correct magnitude indicated by surface measurements. This factor multiplied into radar-computed rainfall rates yielded adjusted rainfall rates which were used in subsequent calculations.

Unfortunately, it is not known for certain exactly how much rain the storm deposited in the area of most severe flooding. No recording raingages were located in this area. A bucket survey of rainfall accumulations for the 48 h period following the onset of the storm, conducted by NWS (Central Region Headquarters in cooperation with other Federal agencies) shows that rainfall totals in the area around Glen Comfort and Glen Haven reached values of 280–300 mm (11–12 inches). This is about five to six times the local average rainfall for the entire month of July.

Data from recording raingages in drainages bordering the Big Thompson suggest that 48 h rainfall accumulations within the NWS bucket survey area consisted of the following parts: 1) rain from the Big Thompson storm, 2) rain from heavy thunderstorms on the evening of the following day and 3) a background of light rain. Rainfall from thunderstorms on the day following the flood could have accounted for as much as 100 mm (4 inches) of the 48 h totals. The lighter rainfall component could have accounted for 25–51 mm (1–2 inches) of the 48 h rainfall accumulation.

No heavy thunderstorms were observed to form in the Big Thompson river drainage on the day following the flood. Only light, upslope rain and low clouds were present. Therefore, only 25–51 mm (1–2 inches) of rain are likely to have fallen in the flood region outside the storm period. The storm rainfall for Glen Comfort was therefore assumed to be 254 mm (10 inches); and this value was used as the normalization to adjust rainfall rates corresponding to various Limon radar intensities.

The following reflectivities were used in calculating total, storm rainfall at Glen Comfort from Limon radar data: 1) the VIP level-2 threshold (30 dBZ), 2) the VIP level-3 threshold (41 dBZ) and 3) a mid-VIP level 3 (44 dBZ). The VIP level 2 was approximated by its threshold valve in order to partially correct for its inflated areal coverage. The mid-VIP level 3 (VIP level 3+) was defined as the central half (in linear dimensions) of any area of VIP level 3.

Three rainfall rates were computed from the reflectivities described above through the Marshall and Palmer (1948) relation

$$Z = 200\,R^{1.6}, \tag{1}$$

where R (mm h^{-1}) is the precipitation rate and Z (mm^6 m^{-3}) the reflectivity factor. The rainfall estimate of 24.8 mm (0.98 inches) for Glen comfort computed from these rainfall rates and the echo time series (Fig. 8) is too low by a factor of 10.2.[6]

Rainfall rates computed for VIP levels 2, 3 and 3+ by means of Eq. (1) were multiplied by the factor 10.2 to yield the adjusted rainfall rates 28, 136, and 210 mm h^{-1}, respectively. The adjusted rainfall rates

[6] The Marshall-Palmer relationship was in operational use by NWS at the time of the flood. Since then, NWS has supplanted this relationship by the equation $Z = 55R^{1.6}$, described by Greene and Clark (1974). This equation leads to an estimate of 56 mm for Glen Comfort which is still low by a factor of about 5.

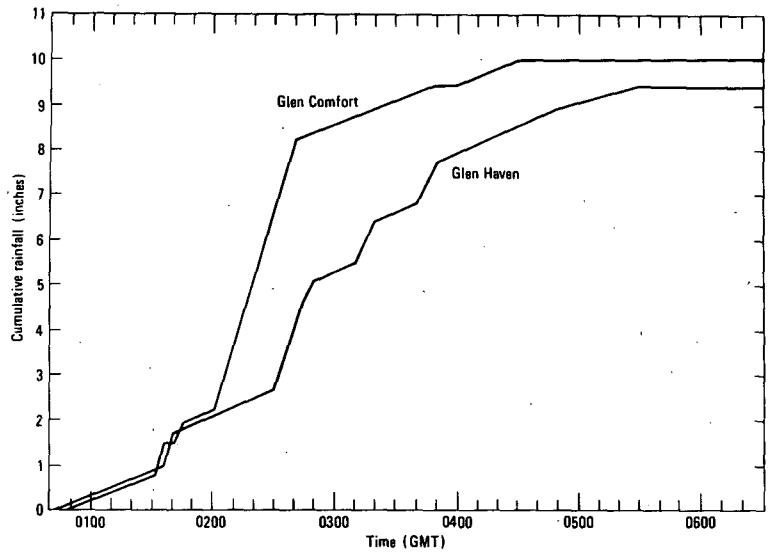

FIG. 9. Accumulated rainfall (inches) estimates for Glen Comfort and Glen Haven, Colorado, from 0040 to 0630 GMT 1 August 1976.

for VIP levels 2, 3 and 3+ correspond to the reflectivities 46, 57 and 60 dBZ, respectively, in Eq. (1). These reflectivities are very consistent with what Grover radar indicated in the radar core areas, but not in the lighter portion of the echo which registered as VIP level 2 on Limon radar.

The radar echo time series (Fig. 8) has been used together with adjusted rainfall rates to generate rainfall accumulation curves for Glen Comfort and Glen Haven (see Fig. 9). Note that at Glen Haven a total rainfall comparable to that at Glen Comfort fell as slightly less intense rain over a longer period of time. The bulk of the rain at Glen Comfort fell in a cloudburst between 0130 and 0240.

b. Distributions of heavy rain

Because the areal coverage Limon radar VIP level 2 was exaggerated, it was not possible to map the entire rainfall pattern of the storm. The heavier rainfall, corresponding to the tighter VIP level 3 and 4 contours, could be estimated, however. (VIP level-4 contours appeared only rarely for only a total of a few minute's duration.) This component of heavy rain intensity is portrayed in terms of isohyets of rainfall accumulation over successive 30 min increments in Fig. 10.

From the isoheyetal pattern it is apparent that the Big Thompson storm complex had two centers of extremely heavy rainfall. Both of these tracked north-northwestward (from ~160° azimuth) at about 2 m s^{-1}. The velocities of these centers were considerably less than the 8–12 m s^{-1} computed for individual cells. Fig. 11 shows the total accumulation of heavy rain from the storm which fell at adjusted rainfall rates corresponding to VIP level 3 or higher. The isohyetal pattern retains the imprint of the two storm centers mentioned above and of the initial burst of heavy rain from 0030 to 0100. Note that the maximum rainfall accumulation in this figure is contoured at 178 mm (7.0 inches). This means that about 70% of the rainfall in this maximum was accumulated under indicated Limon VIP levels 3 and 4. The remaining portion of the rainfall (not included) fell under VIP level-2 reflectivity.

c. Mass rainout rates and precipitation efficiency

Mass rainout rates of that portion of the storm within Limon radar range were also computed assuming that the radar characteristics of the storm did not change significantly during its lifetime. The rainout rates were calculated using areas covered by various VIP levels (measured with a planimeter) in conjunction with adjusted rainfall rates listed in above. A further adjustment was needed however in the precipitation rate corresponding to VIP level 2. The VIP level 2 rainfall rate could not be used throughout because of its areal overestimate. Instead, the effective, VIP level-2 rainfall rate, 11.2 mm h^{-1}, was computed from Grover radar data for about 0100 when Limon radar was indicating reflectivities no higher than VIP level 2. An estimate of the mass rainout rate of the storm based on Grover data was used together with the corresponding area of Limon's VIP level 2 to compute the effective rainfall rate for this inflated portion of the echo.

Mass rainout rates for the storm complex and for that portion of the storm complex within the Big Thompson drainage area are presented in Figs. 12a and 12b, respectively.

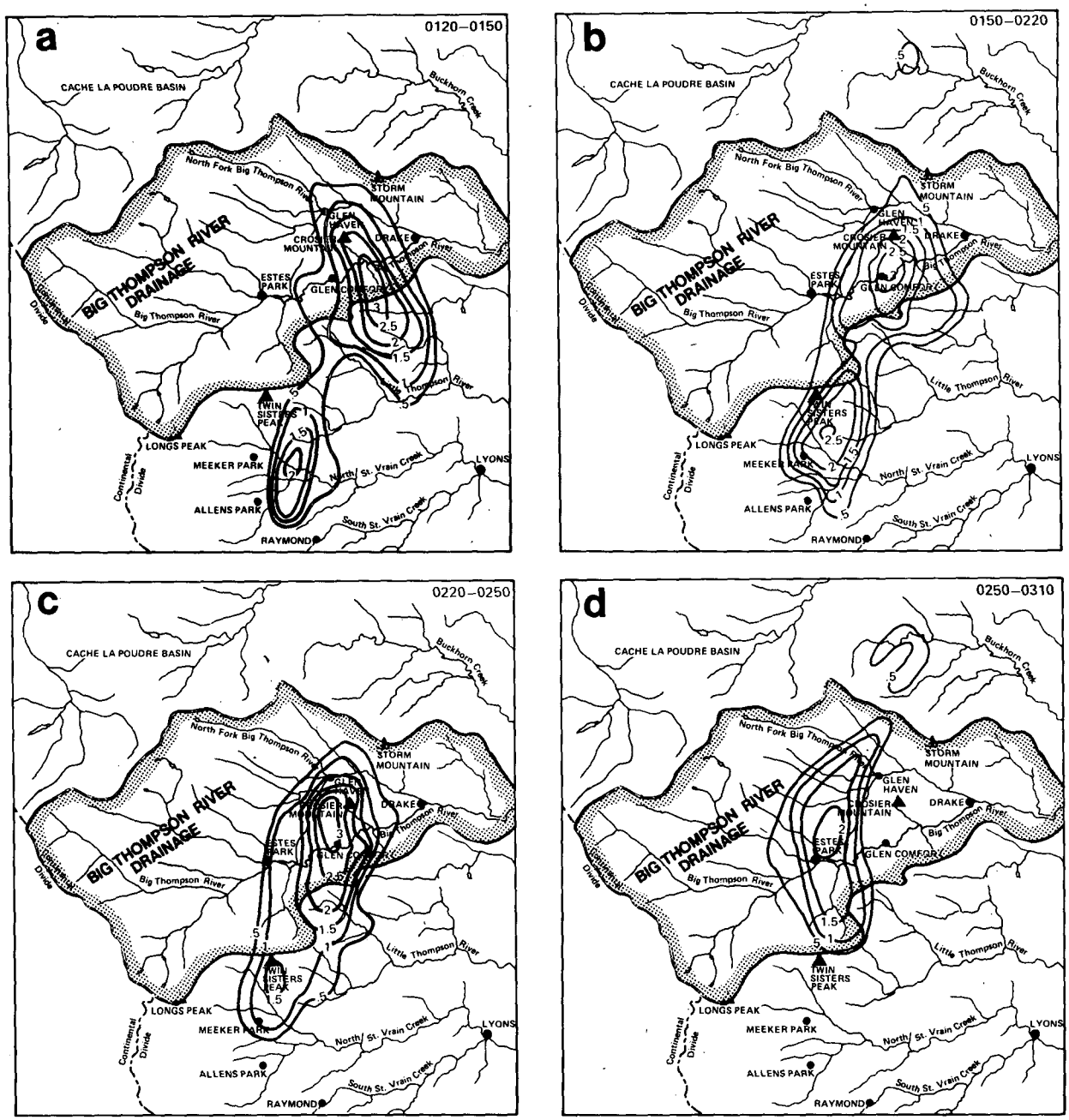

FIG. 10. Isoheyets of heavy rain component (accumulated VIP level 3 or higher) for 30 min intervals from 0120 to 0310 GMT 1 August 1976.

The second curve superimposed on the mass rainout curve in Fig. 12 is a plot of the easterly component of the wind at 600 m AGL over Table Mountain. This curve corresponds to the top of the time-height cross section presented in Fig. 3. The wind-speed curve in Fig. 12a has been offset about an hour to bring it into phase with the rainout curve. Table Mountain was situated about 30 min upwind along the southern boundary of the inflow to the storm. Therefore, half of the offset period can be accounted for as the time required for the moisture bearing winds to reach the Big Thompson area after passing over Table Mountain. The additional 30 min delay perhaps represents the time required to process the moisture into rain.

The rainout of the storm correlates very well with the easterly component of the winds at 600 m AGL over Table Mountain, except during the period from 0050 to 0130 when input into the storm increased while the output of the storm fell dramatically.

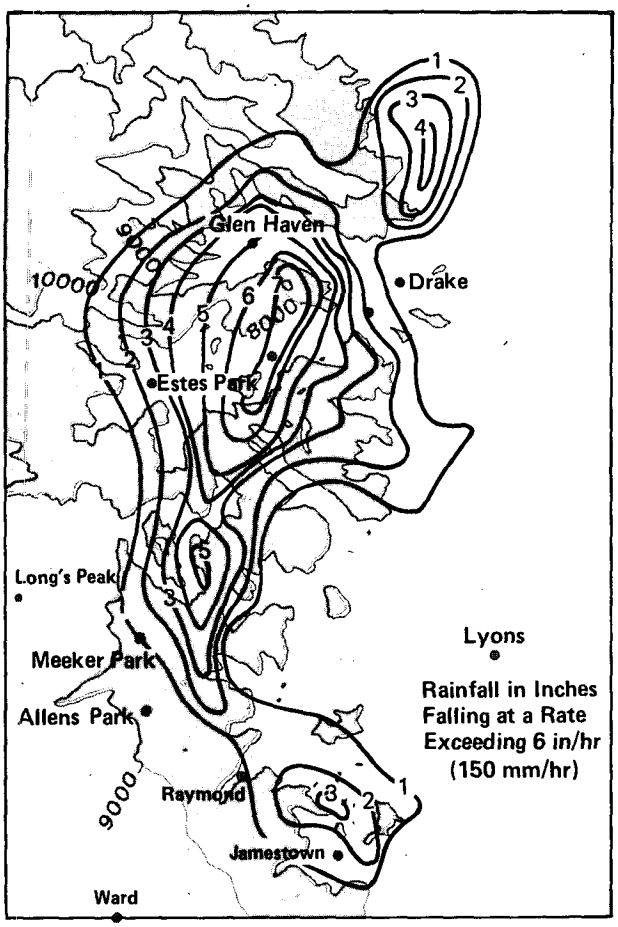

FIG. 11. Heavy rainfall component accumulated throughout the lifetime of the storm from 0000 to 0500 GMT 1 August 1978.

This anomalous period occurred when cold outflow air moved up from the south and apparently interrupted the flow of very moist air into the storm for a brief period.

After the storm reintensified it remained quasi-steady for about 3 h, during which the rainout rate was about 9×10^6 kg s^{-1}. The rainout rates of typical hailstorms reported by Auer and Marwitz (1968) and Foote and Fankhauser (1973) average about 2×10^6 kg s^{-1}. A rainout rate of 9×10^6 kg s^{-1} is more like that of a giant squall-line thunderstorm for which Newton (1966) estimated a moisture flux of 8.8×10^6 kg s^{-1} with a residual of about 4.0×10^6 kg s^{-1} reaching the surface as precipitation. Considerable rainfall was lost in Newton's case through evaporation in the downdraft.

The efficiency of the Big Thompson storm can be estimated by using the Table Mountain data (Fig. 3) and the interpolated Loveland sounding (Fig. 5b). The inflow layer was about 1.4 km thick with a mean mixing ratio of 14.8 g kg^{-1} and a mean easterly component of inflow velocity of about 17 m s^{-1}. The north-south extent of the storm was taken to be 30 km. Low-level moisture flux into the storm is then computed to be about 10.6×10^6 kg s^{-1} which is close to the rainout rate of 9×10^6 kg s^{-1}. From this rough calculation it appears that the precipitation efficiency of the storm was about 85%. The Big Thompson storm achieved high efficiencies because evaporational losses were minimal and convective-scale downdrafts were largely absent.

The high precipitation efficiency of the Big Thompson is consistent with the inverse relation between in-cloud shear and precipitation efficiency for Great Plains thunderstorms (Marwitz, 1972). It must be remembered, however, that the Big Thompson storm developed within an environmental wind structure that was quite different than that usually associated with Great Plains thunderstorms.

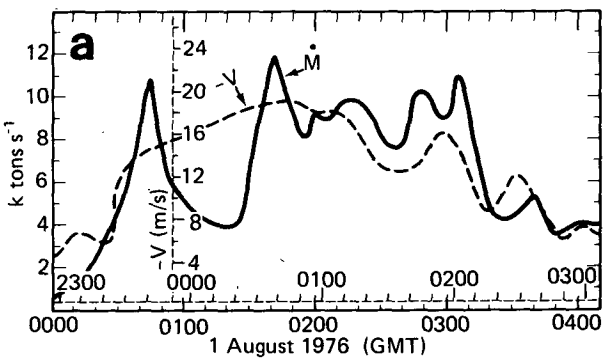

FIG. 12a. Mass rainout rate from the storm (solid curve) from 0000 to 0400 GMT 1 August 1976. The dashed curve is the easterly component of the wind at 600 m AGL above Table Mountain.

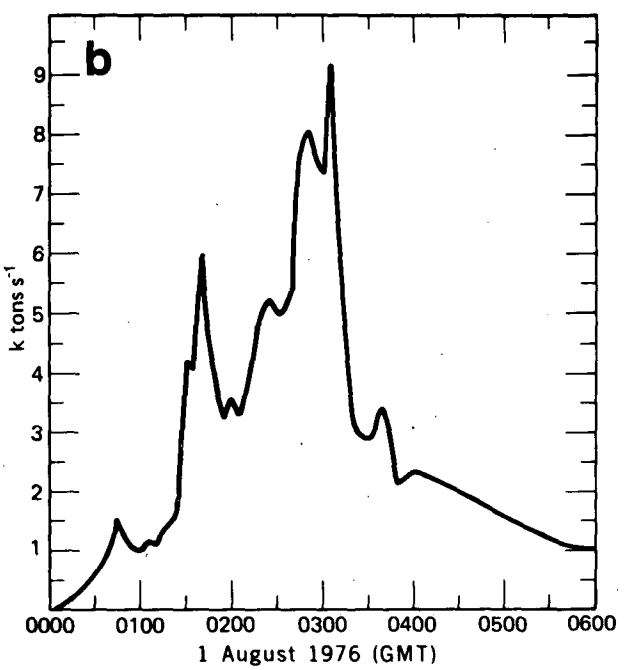

FIG. 12b. Mass rainout rate at that portion of the storm within the Big Thompson river drainage.

5. Physical model of the storm

Grover radar data was used to construct a vertical cross section of one of the first cells of the Big Thompson storm along the direction of inflow (Fig. 13a). The structure of this cell was much different from that of a severe thunderstorm over the Great Plains as typified by the Fleming storm (Fig. 13b). The cell shown in Fig. 13a remained nearly stationary along the southeastern slopes of Storm Mountain. An important feature of the vertical structure of this cell is that it had a low-echo-centroid (LEC) i.e., its highest reflectivities were located within the warm portion of the cloud (below 7 km, MSL). In contrast, the Fleming storm had high reflectivity extending well into the glaciated portion of the cloud.

The environmental winds depicted in Figs. 13a and 13b show that both the Big Thompson storm and the Fleming storm formed in a sheared environment. Although the vertical wind shear vector was similar in both cases, it was produced in entirely different ways relative to the surface. The environmental winds showed very little shear across the Big Thompson storm from cloud base to cloud top. The shear in this case was mainly confined to the boundary layer and near cloud base where strong southeasterly flow moving under relatively light upper level winds from the south produced a reverse shear. In the case of the Fleming storm, however, the cloud itself was strongly sheared throughout its depth. Reverse shear is typical of a cloudburst situation and is responsible for a great

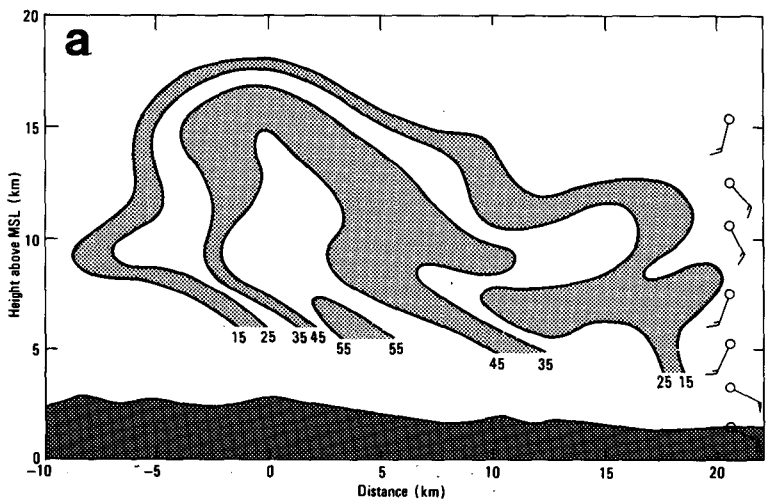

FIG. 13a. Grover radar reflectivity (dBZ) cross section through one of the initial cells of the Big Thompson storm complex at 0045 GMT. Winds (kt) are from the Loveland, Colorado, interpolated sounding. Cross section was orientated from 314° to 134° through a point at 40°30'N and 105°12'W. Cross section lies nearly along storm inflow.

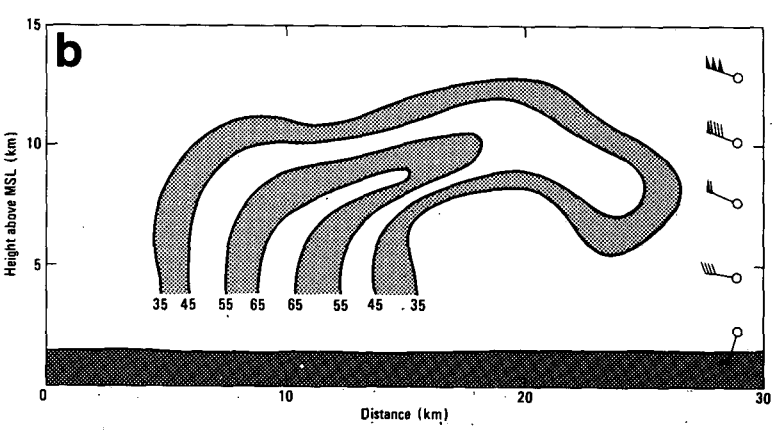

FIG. 13b. Grover radar reflectivity (dBZ) cross section through the severe Fleming, Colorado, hailstorm (after Browning and Foote, 1975). Winds (in knots) are from a nearby upper air sounding. Cross section lies nearly along storm inflow.

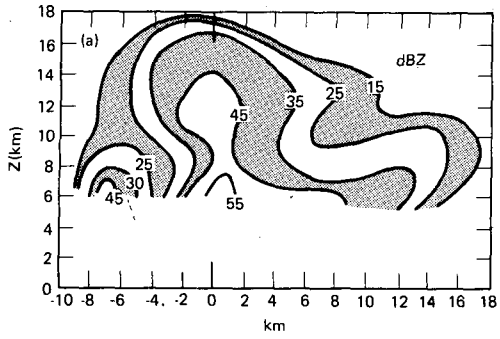

FIG. 14a. Grover radar reflectivity (dBZ) cross section through the same cell as in Fig. 13a but at 0100 GMT. Cross section was oriented from 314° to 134° through the center of the reflectivity core which was now located slightly west of earlier location. Direction of inflow was from right to left.

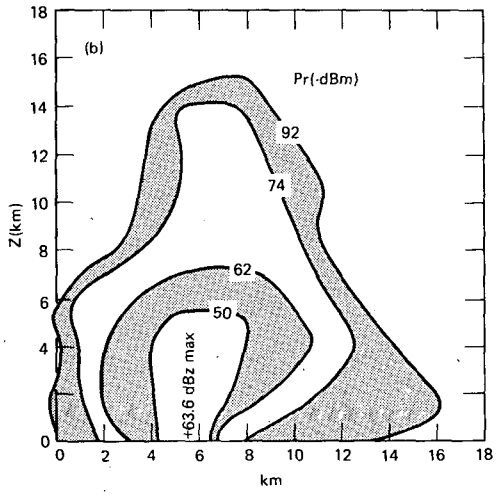

FIG. 14b. Radar reflectivity cross section through an Indian monsoon thunderstorm adapted from Maheshwari and Mathur (1968). Direction of low level inflow is from left to right.

measure of the high precipitation efficiencies achieved by these storms.

The LEC structure of the Big Thompson storm is apparently rare along the eastern slopes of the Rocky Mountains and the Great Plains. This structure, however, seems to be common in the tropics. Recently published RHI radar cross sections of tropical squall-line cumulonimbi (see Houze, 1977) show LEC structures. Monsoon thunderstorms in India typically show this structure in having their peak radar reflectivities at or below the freezing level (Maheshwari and Mathur, 1968). Notice the similarity between the RHI radar cross sections of the Big Thompson storm (Fig. 14a) and of a monsoon thunderstorm (Fig. 14b).

Grover radar data taken at 0045 and the interpolated Loveland sounding were used to formulate a physical model of the Big Thompson storm during its mature and nearly steady-state period. The storm model, shown in Fig. 15, was drawn to conform to the echo depicted in Fig. 13a. The structure of this cell is believed to typify the mature Big Thompson storm because, unlike many of the initial cells, it became almost stationary.

A strong low-level inflow (~1.4 km thick and with a mean mixing ratio of ~14.8 g kg^{-1}) produced a strong moisture flux into the storm area. On approaching the Front Range the storm inflow was lifted above the LCL (about 2.5 km MSL). Stratus and stratocumulus clouds formed in the 80 mb thick layer between cloud base and the LFC. The 0000 Fort Collins surface observation indicated a thin, broken-cloud deck based at 1.2 km AGL (4000 ft).

At some point along the mountainous topography the airmass was forced above the LFC and vigorous convection developed. New cells formed in the inflow and propagated north-northwestward into the stationary storm complex where cloud base was effectively on the ground. Similar features were also characteristic of the Rapid City storm (Dennis *et al.*, 1973).

Schroeder's (1977) conceptual model of a flood-producing thunderstorm over the Koolau Range in Hawaii is similar to the Big Thompson model (Fig. 15), indicating that this type of storm is probably not unique to the Front Range area but that it can occur anywhere that strong, very moist, boundary-layer winds are directed upslope into mountainous terrain or over cold mesohighs produced by preexisting thunderstorms.

The model of the Big Thompson storm depicted in Fig. 15 is considerably different from that developed by St. Amand *et al.* (1972) for the Rapid City, South Dakota, storm complex. Their model cloud sloped strongly to the east above 450 mb and invoked a recycling of water substance to help explain the high precipitation efficiency of the system. A towering cumulus cloud over flat terrain that develops within an airmass having reverse shear will normally tend to slope toward the east with height. The lower portion of the cloud moves faster toward the west than the middle and upper levels. With orographic convective storms in reverse shear, however, the lifting required to trigger the instability effectively anchors the lower portion of the cloud on the mountains. The vertical transport of strong easterly momentum into the storm then produces an updraft structure that slopes along the direction of inflow. Grover radar data suggest that cells moving toward the west, tilted toward the east with height; whereas those with little westward motion tilted toward the west with height. In the mature Big Thompson storm, the westward tilted updraft allowed large precipitation droplets to fall out of the rear of the updraft, enabling the system to exist in a nearly steady state.

The efficient unloading of liquid water from the

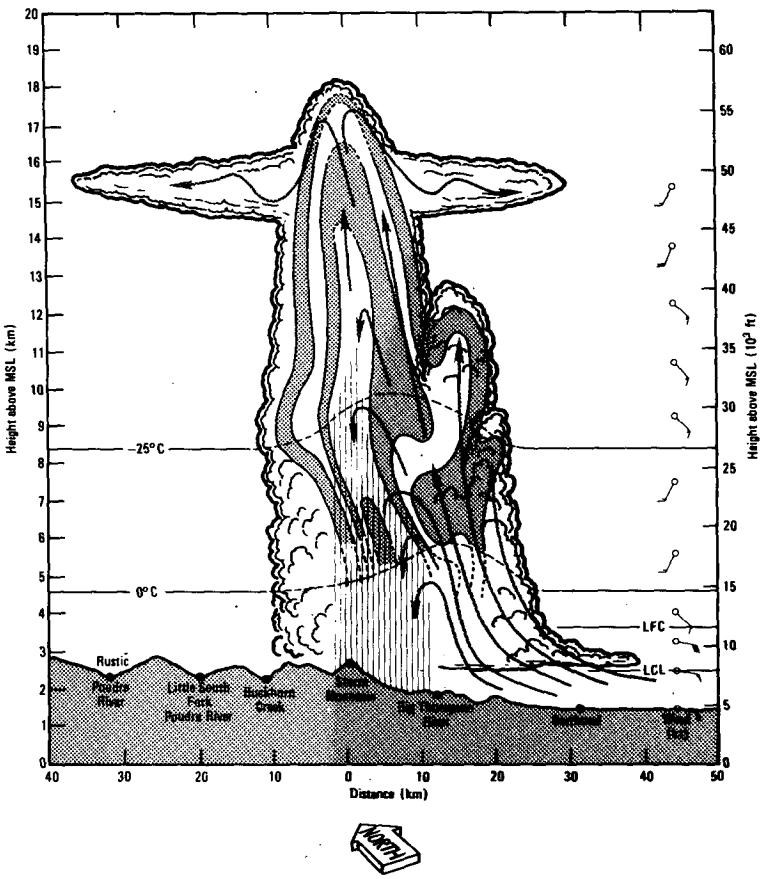

FIG. 15. Physical model of one of the initial cells of the Big Thompson storm complex. LCL, LFC, winds and levels of 0°C and −25°C isotherms are from interpolated Loveland, Colorado, sounding. Grover 0045 GMT radar reflectivities are shown with 10 dBZ contours beginning with 15 dBZ level.

lower portion of the cloud would enhance updraft speeds in upper portions of the cloud, and at the same time, suppress hail growth in the supercooled portions of the updraft. The overall effect would be to produce high echo tops, little echo overhang, and an LEC. These characteristics of the model are confirmed by the available radar observations and eye witness accounts.

The LEC structure of the Big Thompson storm and lack of appreciable hail give evidence that warm rain processes played an important part in generating storm precipitation. In Fig. 15 the high in-cloud freezing level (5.8 km MSL), the height of the −25°C isotherm (9.6 km MSL) and low cloud base (2.5 km MSL) indicate a deep layer (3–7 km thick) for warm cloud coalesence processes to act. The highest storm reflectivities developed and remained well below the −25°C isotherm. The layer of warm cloud in this storm was thicker than in Hawaiian cumulus clouds, which often produce rains rivaling those of the Great Plains thunderstorm through warm cloud processes in clouds only 3 km thick (Rodgers, 1966). Since the highest reflectivities of the Big Thompson storm centered in the warm cloud, it is very probable that the major portion of precipitation grew in this portion of the cloud.

Only light hail falls (marble size and smaller) were reported by eyewitnesses to have occurred from the first cells of the Big Thompson storm between 0030 and 0100. In the core of the storm, during the cloudburst period, however, there was no mention of hail. This is another feature which the mature Big Thompson storm had in common with monsoon thunderstorms where "hail is conspicuous by its absence" (Maheshwari and Mathur, 1968), and with the storm which caused the Rapid City flood (Dennis *et al.*, 1973).

The lack of appreciable hail and strong in-cloud wind shear cooperated to enhance the precipitation efficiency of the storm by suppressing the development of organized, convective-scale downdrafts. The downdraft circulation can consume a substantial amount of the potential precipitation in the evaporative cooling of subsiding air. In the giant squall-line thunderstorm analyzed by Newton (1966) roughly half of the potential precipitation was con-

sumed within the downdraft. In the case of the Big Thompson storm, lifting provided by mountainous terrain, lack of appreciable hail fall and cloud bases very near the surface acted to minimize the downdraft circulation. Therefore, cool outflow did not spread eastward out of the mountains to trigger new convective cells further east. This allowed the Big Thompson storm to remain quasi-stationary for a few hours. Again the lack of strong downdrafts was also a feature of the flood producing storm at Rapid City (Dennis *et al.*, 1973).

The LEC structure of the Big Thompson storm partially accounts for the failure of the Limon radar to resolve the true intensity of the Big Thompson storm. The center of the radar beam (which was ~7 km in diameter) scanned the storm at about 6 km MSL (19 700 ft). Nearly half the beam extended above the high-reflectivity cores into weaker reflecting portions of the cloud. The Limon radar registered the presence of these high-reflectivity cores as areas of VIP level 3 with brief flashes of VIP level 4. The strong reflectivity gradients across the beam caused the Limon radar to indicate a much weaker reflectivity maxima than would have been indicated by a radar with a higher beam resolution scanning below 7 km MSL. The primary clue to storm's severity was furnished by Limon cloud top measurements which disclosed overshooting storm tops towering above 18.3 km (60 000 ft) MSL, about 1.8 km (6000 ft) higher than any of the other storms in the eastern slopes and plains.

An RHI scan of the Rapid City storm contained in a report by St. Amand *et al.* (1972) strongly suggests an LEC structure also. The Big Thompson and Rapid City storms appear to have a strong kinship with a type of orographic storm that is common in the tropics and apparently rare in the Great Plains and Rocky Mountains. Because warm cloud processes predominate in forming precipitation, the highest storm reflectivities are situated in the warm portions of the cloud. In contrast severe storms over the Great Plains normally form precipitation predominantly through ice processes. High reflectivities usually extend well into the glaciated portion of the cloud.

Because of their elevated echo structure, Great Plains thunderstorms often produce strong radar echoes at large distances on WSR-57 radars. Radar meteorologists have tended to judge the severity and rainfall rate of such storms at long range from their observed radar echoes, because usually there are no problems associated with vertical beam resolution. The LEC type storm, however, may present deceptively weak radar echoes especially at long distances where the major portion of the radar beam may pass above the strongest reflecting portion of the cloud.

6. Summary and Conclusions

A large quasi-stationary storm complex was spawned over the mountainous terrain drained by the Big Thompson river as potentially very unstable air flowed westward behind a secondary frontal surge. The potentially unstable air was capped by a frontal inversion, which suppressed convection over the plains. As the air mass reached the eastern slopes of the Front Range, orographic lifting provided the necessary destabilization to trigger convection. The stable flow behind the front then continued to feed the storm complex. The location of the storm along the Front Range coincided with the mesoscale focusing of the moisture flux into the Big Thompson area.

It appears that atmospheric conditions on several scales, including cloud microphysical processes, acted in harmony to produce storms with precipitation efficiencies much higher than is typical of Great Plains thunderstorms. The stationary inflow and fixed topography together with a very light upper level flow (with a component toward the mountains) acted in tandem to maintain a quasi-stationary storm. Because of the vertical transport of horizontal easterly momentum the storm complex organized with an overall tilted updraft structure. Dynamical, thermodynamical and microphysical processes worked in harmony to produce a nearly steady-state storm complex. A high moisture flux coupled with a high precipitation efficiency combined to produce torrential rains for several hours.

Rain apparently grew mainly through warm cloud coalescence processes and reached torrential rainfall rates. This gave the storm a low-echo-centroid which limited the distance over which operational weather radar could resolve the high-reflectivity cores. A WSR-57 scanning the storm from a range greater than 100 n mi had anomalously weak echoes returned from the storm because of the lack of vertical beam resolution. The only clue to the storm's true intensity was in its high overshooting tops.

Acknowledgments. The authors would like to thank the many persons and organizations who supplied data used in this study. The Department of Atmospheric Science, Colorado State University, provided data for Ft. Collins. Dr. C. Glenn Cobb supplied Greeley data measured at Ross Hall, University of Northern Colorado. John M. West of Rockwell International Corp. supplied the Rock Flats data, and Frank Pratte of Wave Propagation Laboratory (NOAA–ERL) provided the data from Table Mountain. James F. W. Purdom of NOAA–NESS Applications Group supplied copies of GOES imagery. The NHRE and the National Center for Atmospheric Research Field Observing Facility

obtained and supplied the invaluable sounding, radar and surface data from the NHRE site in northeastern Colorado. National Climatic Center (NOAA–EDS) personnel expeditiously filled several large data requests. John Asztalos of Waukesha, Wisconsin, provided copies of photographs that he had taken of the developing storm.

REFERENCES

Auer, A. H., Jr., and J. D. Marwitz, 1968: Estimates of air and moisture flux into hailstorms on the High Plains. *J. App. Meteor.*, **7**, 196–198.

Browning, K. A., and G. B. Foote, 1976: Airflow and hail growth in supercell storms and some implications for hail suppression. *Quart. J. Roy. Meteor. Soc.*, **102**, 499–533.

Dennis, A. S., R. A. Schleusener, J. H. Hirsch and A. Koscielski, 1973: Meteorology of the Black Hills flood of 1972. Rep. 73-4, Institute of Atmos. Sci., South Dakota School of Mines and Technology, 41 pp.

Foote, G. B., and J. C. Fankhauser, 1973: Air and moisture budget beneath a northeast Colorado hailstorm. *J. Appl. Meteor.*, **12**, 1330–1353.

Greene, D. R., and Clark, R. A., 1974: The operational use of digital radar data for flash-flood monitoring. *Symposium on Flash Floods, Tercentenary of Scientific Hydrology*, IAHS-AISH Publ. No. 112, 100–115.

Houze, R. A. Jr., 1977: Structure and dynamics of a tropical squall-line system, *Mon. Wea. Rev.*, **105**, 1540–1567.

Maddox, R. A., F. Caracena, L. R. Hoxit, and C. F. Chappell, 1977: Meteorological aspects of the Big Thompson flash flood of 31 July 1976. NOAA TR ERL 388-APCL 41, 83 pp.

——, L. R. Hoxit, C. F. Chappell and F. Caracena, 1978: Comparison of meteorological aspects of the Big Thompson and Rapid City flash floods. *Mon. Wea. Rev.*, **106**, 375–389.

Maheshwari, R. C., and I. C. Mathur, 1968: Radar reflectivity studies of Indian summer monsoon over Northwest India. *Preprints 13th Radar Meteorology Conf.*, Montreal, Amer. Meteor. Soc., 98–103.

Marshall, J. S., and W. M. K. Palmer, 1948: The distribution of raindrops with size. *J. Meteor.*, **5**, 165–166.

Marwitz, J. D., 1972: Precipitation efficiency of thunderstorms on the High Plains. *J. Rech. Atmos.*, **6**, 367–370.

Newton, C. W., 1966: Circulations in large sheared cumulonimbus. *Tellus*, **18**, 699–713.

Rodgers, R. R., 1967: Doppler radar investigations of Hawaiian rain. *Tellus*, **19**, 432–455.

St. Amand, P., R. J. Davis, and R. D. Elliot, 1972: Report on Rapid City flood of 9 June 1972. Report to South Dakota Weather Control Commission, Pierre, SD, 37 pp.

Schroeder, T. A., 1977: Meteorological analysis of an Oahu flood. *Mon. Wea. Rev.*, **105**, 458–468.